Electronic Supplementary Material (ESI) for Journal of Materials Chemistry C.

Supporting Information

Oxygen vacancy-rich, Ru-doped In_2O_3 ultrathin nanosheets for efficient detection of xylene at low temperature

JinWang[a#], Juan Su [b#], Hui Chen[a], Xiaoxin Zou[a], Guo-Dong Li[a]*

[a]State Key Laboratory of Inorganic Synthesis and Preparative Chemistry, College of Chemistry, Jilin University, Changchun 130012, P.R. China

[b]School of Chemistry and Chemical Engineering, Shanghai Jiao Tong University, Shanghai 200240, P. R. China

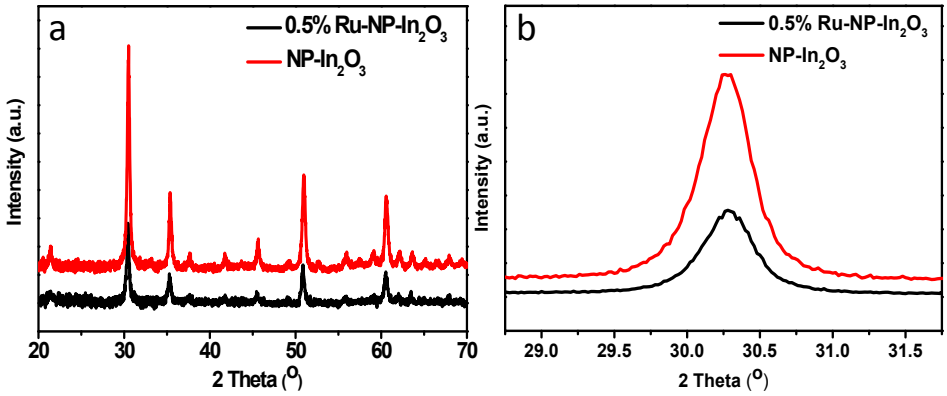

Figure S1 (a) XRD patterns for NP-In_2O_3 and 0.5% Ru-NP-In_2O_3, (b) Amplified XRD patterns from 28.75 to 31.75 degree.

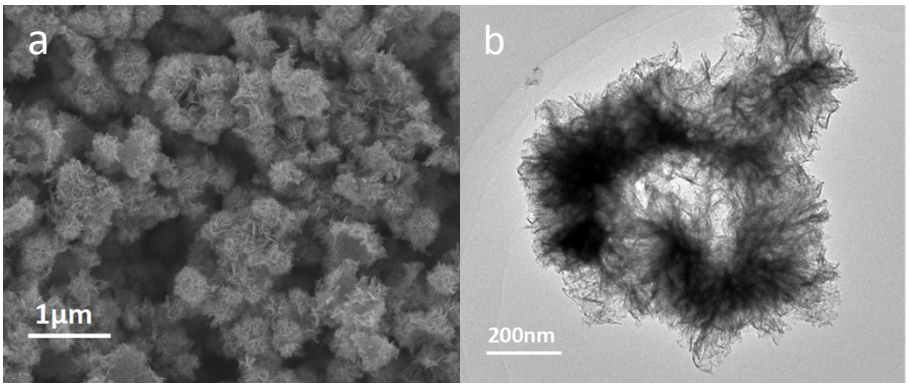

Figure S2 (a) SEM and (b) TEM images of In-NS.

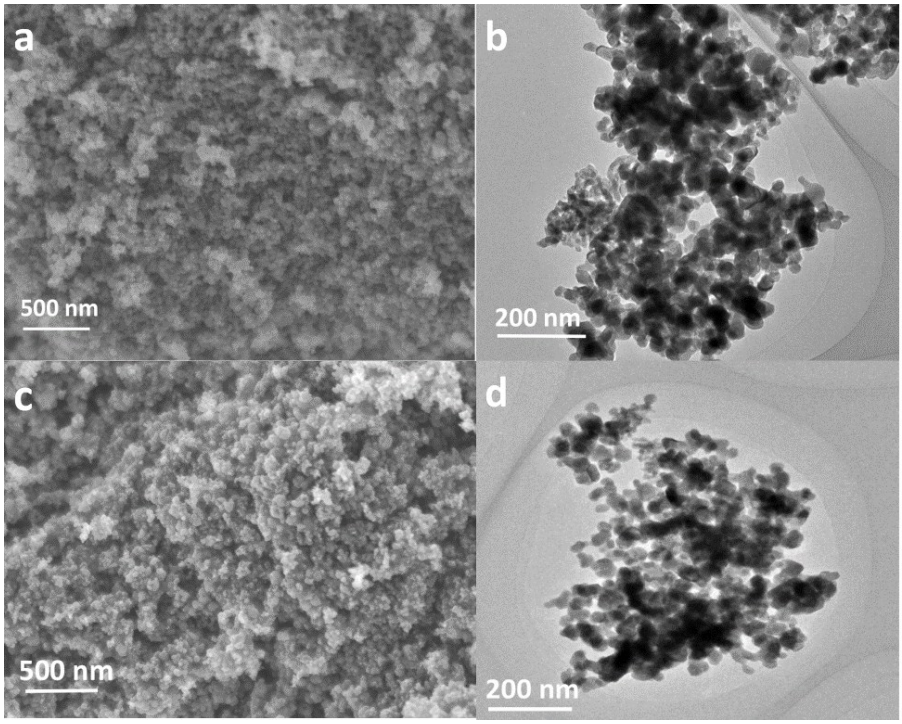

Figure S3 (a) SEM and (b) TEM images of NP-In_2O_3, (c) SEM and (d) TEM images of 0.5% Ru-NP-In_2O_3.

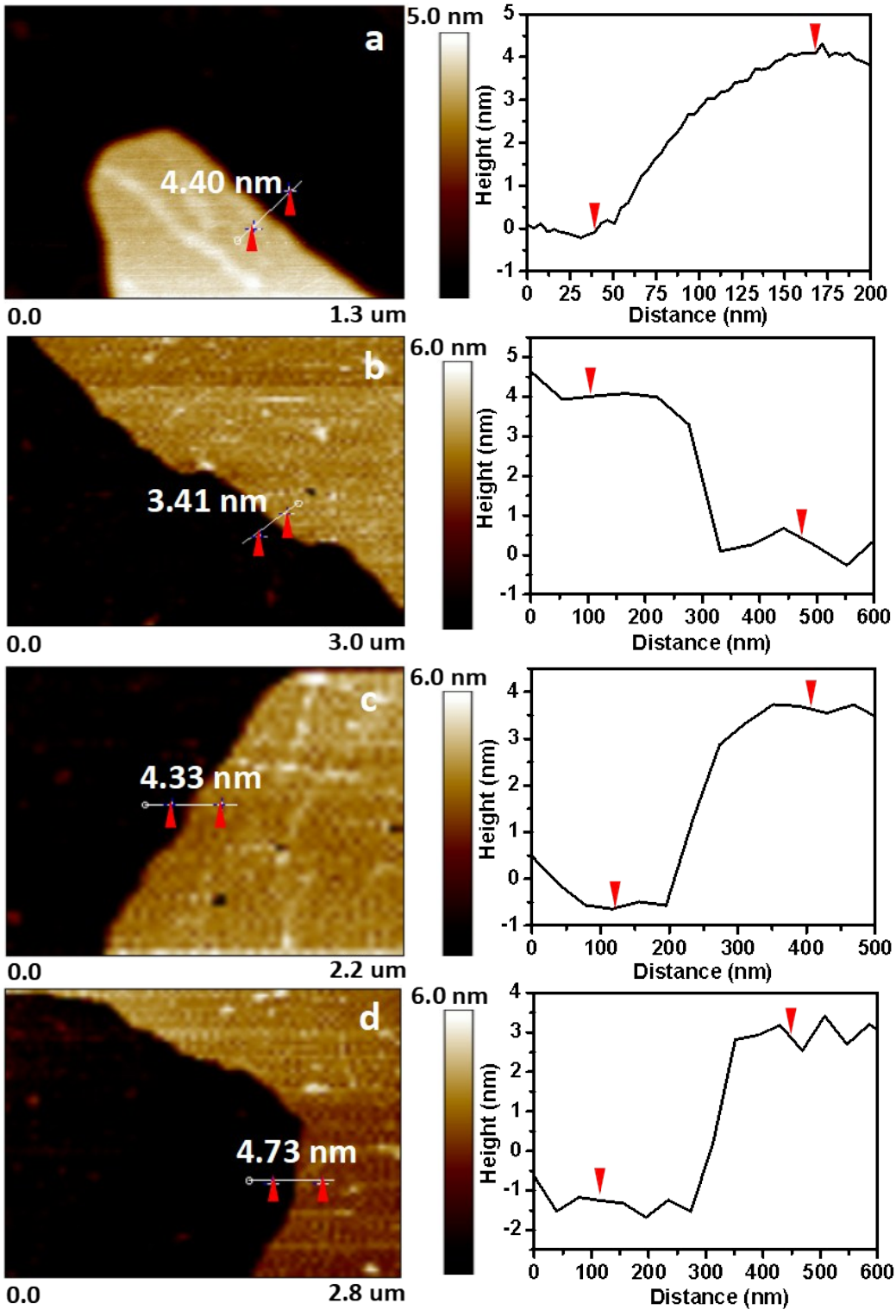

Figure S4 AFM images of (a) In-NS, (b) In_2O_3, (c) 0.25% Ru-In_2O_3 and (d) 1% Ru-In_2O_3.

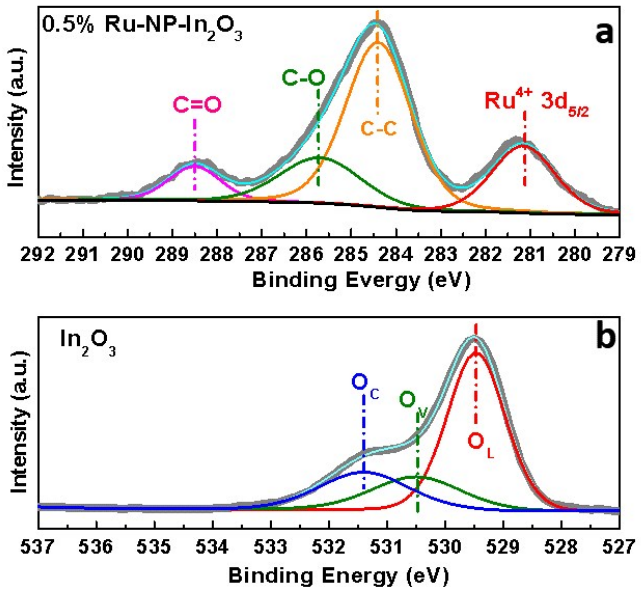

Figure S5 (a) The Ru 3d XPS spectra for 0.5% Ru-NP-In_2O_3 and (b) The O 1s XPS spectra for In_2O_3.

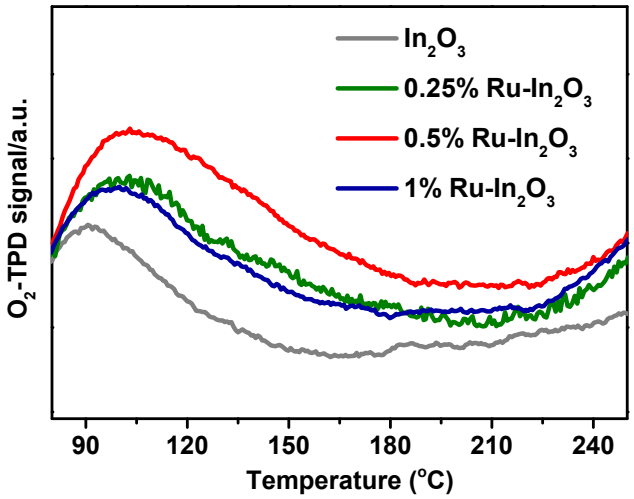

Figure S6 Temperature-programmed oxygen desorption curve (O_2-TPD) for In_2O_3, 0.25% Ru-In_2O_3, 0.5% Ru-In_2O_3 and 1% Ru-In_2O_3.

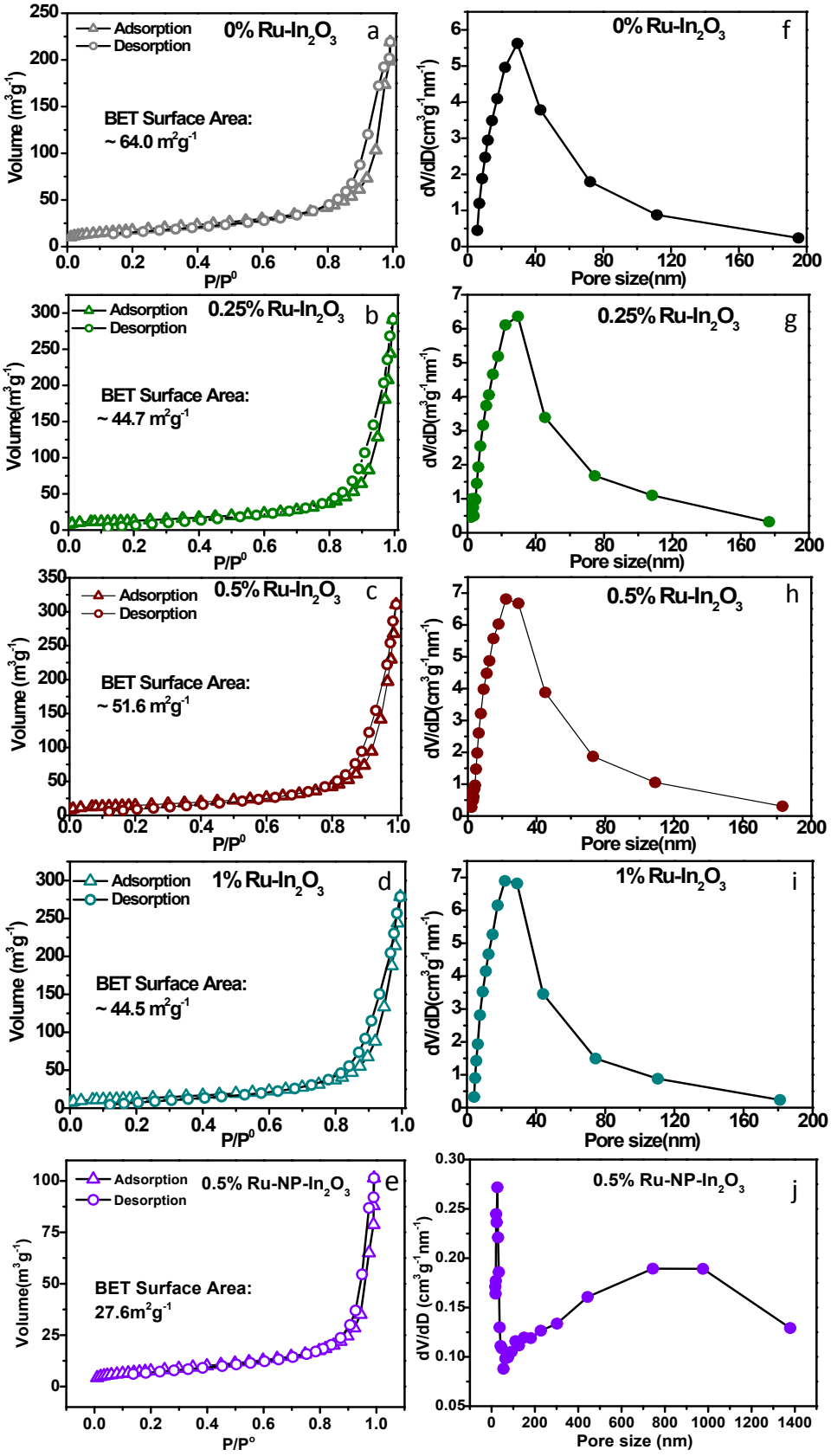

Figure S7 (a-d) The N_2 adsorption–desorption isotherms and (e-h) pore size distribution for In_2O_3, 0.25% Ru-In_2O_3, 0.5% Ru-In_2O_3, 1% Ru-In_2O_3 and 0.5% Ru-NP-In_2O_3.

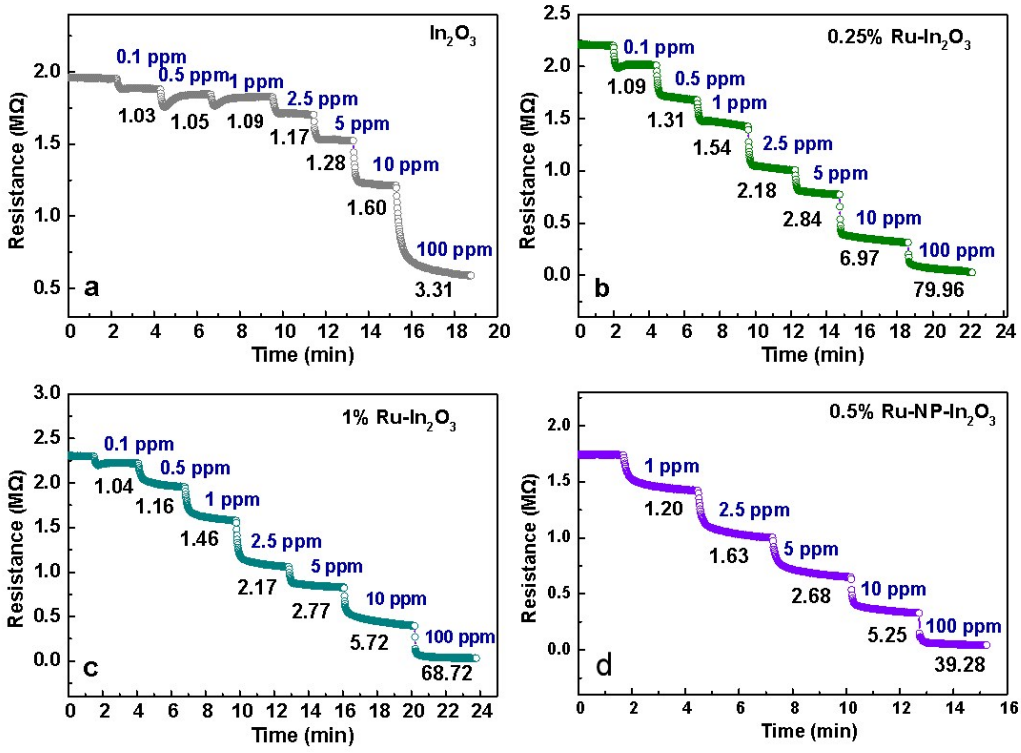

Figure S8 Dynamic xylene sensing transients of (a) In_2O_3, (b) 0.25% Ru-In_2O_3, (c) 1% Ru-In_2O_3 and (d) 0.5% Ru-NP-In_2O_3 at 120°C.

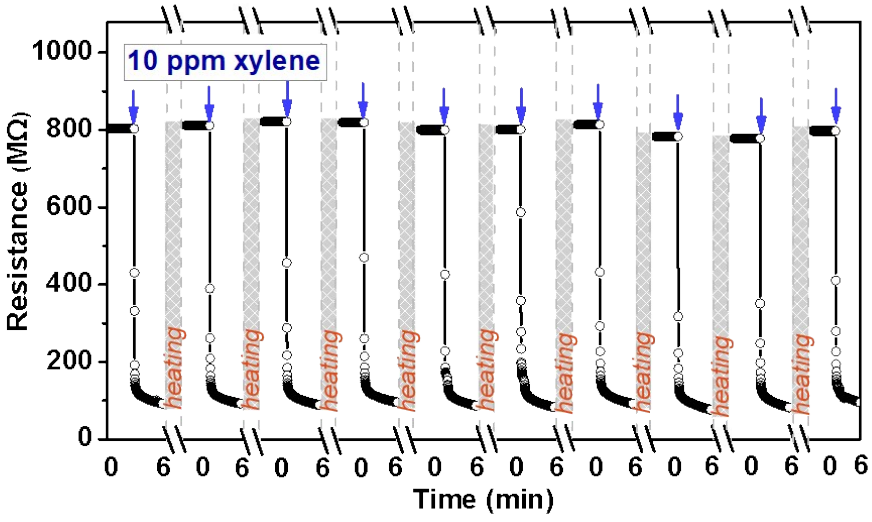

Figure S9 The response−recovery of 0.5% Ru-In_2O_3 toward 10 ppm xylene gas for 10 cycles at 120°C and 210°C, respectively.

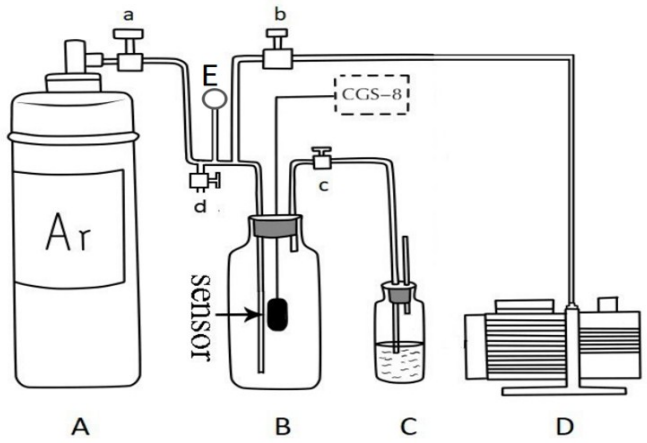

Figure S10 The diagram for oxygen free test.

The procedure of oxygen free test

The oxygen free test device is composed by an argon cylinder (A), a test chamber (B), a safety bottle filled with methyl silicone (C), a vacuum pump (D) and a vacuum meter (E). Firstly, the valve (a), (c) and (d) were turned off and the valve (b) was turned on, then D could evacuate air from B. At this moment, the resistance of the sensor went down a little. When the resistance of the sensor didn't change, valve (b) was blocked off. Subsequently, the valve (a) was opened, making argon gas to get into B, till the pressure of B was a about $1/100^{th}$ higher than normal atmosphere as shown in meter (E). Then, valve (a) was turned off and valve (c) was turned on carefully to reduce the pressure of B to normal atmosphere. Taking about one hour, the resistance of the sensor will be stable. To remove oxygen from B as far as possible, this process should be repeated for three times. Finally, the resistance of the sensor decreased to one-twelfth as that of the sensor in air, named as R_{ar}.

The resistance of the sensor in argon is defined as R_{ar}, which is reduced to about 154.0 kΩ. Next, all valves were turned off and a certain quantity of xylene liquid was injected into B. The resistance of the sensor will be decreased. After 10 minutes, the resistance of the sensor became stable again, the resistance is defined as R_{xy}.

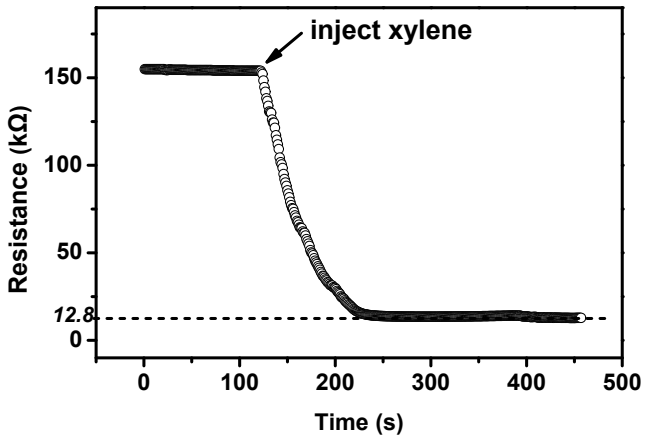

Figure S11 The resistance change of 0.5% Ru-In_2O_3 sensor for oxygen free test.

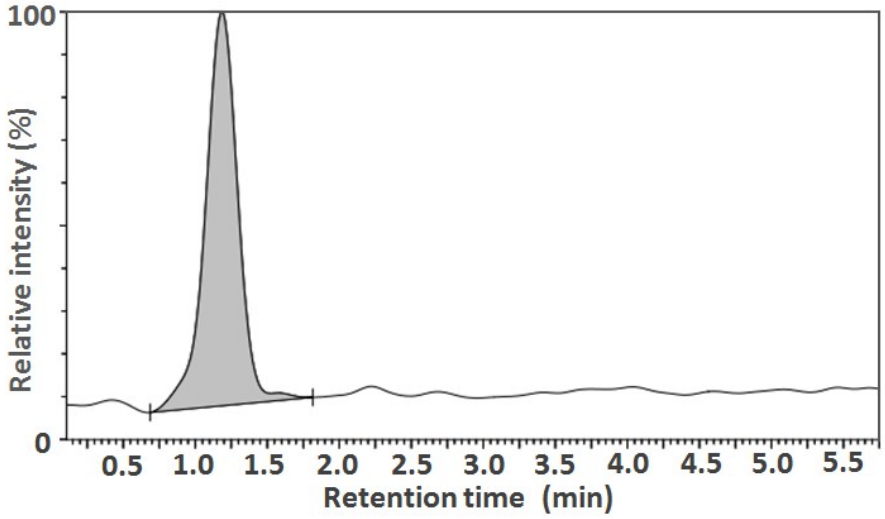

Figure S12 UHPLC chromatogram of the xylene oxidation product at 120 °C.

Table S1 Atom ratio of O_L, O_V and O_C for In_2O_3 and 0.25% Ru-In_2O_3, 0.5% Ru - In_2O_3, 1% Ru-In_2O_3 and 0.5% Ru-NP-In_2O_3.

Samples	Atom ratio of O_L (%)	Atom ratio of O_V (%)	Atom ratio of O_C (%)	Atom ratio of Ru^{3+} (%)	Atom ratio of Ru^{4+} (%)
In_2O_3	59.38	19.02	21.60	0	0
0.25%Ru-In_2O_3	27.73	23.22	49.04	74.4	25.6
0.5%Ru-In_2O_3	6.33	28.74	64.93	55.7	44.3
1%Ru-In_2O_3	23.26	25.45	51.29	84.9	15.1
0.5%Ru-NP-In_2O_3	59.48	6.48	28.84	0	100

Table S2 BET surface area of In_2O_3, 0.25% Ru-In_2O_3, 0.5% Ru-In_2O_3, 1% Ru-In_2O_3 and 0.5% Ru-NP-In_2O_3.

Samples	In_2O_3	0.25% Ru-In_2O_3	0.5% Ru-In_2O_3	1% Ru-In_2O_3	0.5% Ru-NP-In_2O_3
BET surface area (m^2/g)	64.0	44.7	51.6	44.5	27.6

Table S3 The summary of xylene sensing performance reported previously and this work.

NO.	Materials	Xylene (Conc.)	Temp. (°C)	Response (R_a/R_g)	Ref.
1	**Ru-In_2O_3 nanosheets**	**100 ppm**	**120**	**128.9**	**This work**
2	Cr-doped Co_3O_4	100 ppm	139	12	[1]
3	Flower-like Co_3O_4	100 ppm	150	79.8	[2]
4	CuO nanostructures	100 ppm	260	2.4	[3]
5	$Fe_2(MoO_4)_3$ nanoplates	100 ppm	340	25.9	[4]
6	Co_3O_4 nanorod arrays	100 ppm	160	~31	[5]
7	ZnO nanoflowers	100 ppm	200	~6	[6]
8	Au/MoO_3 hollow spheres	100 ppm	250	22.1	[7]
9	ZnO/$ZnCo_2O_4$ hollow core–shell nanocages	100 ppm	320	35	[8]
10	Co_3O_4 nanocubes	100 ppm	200	~6.5	[9]
11	SnO_2 porous microcubes	100 ppm	240	10.7	[10]
12	α-Fe_2O_3/Bi_2WO_6	100 ppm	260	13.5	[11]
13	Pd-doped WO_3nanocube	100 ppm	230	~50	[12]
14	WO_3 nanolamella	100 ppm	280	47	[13]
15	ZnO/$Ni_{0.9}Zn_{0.1}O$ double-shelled nanocages	100 ppm	240	~55	[14]
16	Fe doped Co_3O_4	100 ppm xylene	175	18.2	[15]
17	Fe-doped MoO_3 nanobelts	100 ppm xylene	206	6.1	[16]
18	Co_3O_4 microspheres	100 ppm xylene	150	74.5	[17]
19	Cr_2O_3@WO_3 nanostructures	100 ppm	300	26.6	[18]
20	Ni doped TiO_2	100 ppm	302	~3.5	[19]

References for SI

1. Y. Li, X. Ma, S. Guo, B. Wang, D. Sun, X. Zhang and S. Ruan, *RSC Adv.*, 2016, **6**, 22889-22895.
2. K. Xu, L. Yang, J. Zou, Y. Yang, Q. Li, Y. Qu, J. Ye and C. Yuan, *J. Alloys Compd.*, 2017, **706**, 116-125.
3. C. Yang, F. Xiao, J. Wang and X. Su, *Sens. Actuators, B*, 2015, **207**, 177-185.
4. M. Xu, Z. Lin, W. Guo, Y. Hong, P. Fu, Z. Chen and D. Tang, *Funct. Mater. Lett.*, 2017,**10**, 1750022.
5. Z. Wen, L. Zhu, W. Mei, Y. Li, L. Hu, L. Sun, W. Wan and Z. Ye, *J. Mater. Chem. A*, 2013, **1**, 7511-7518.
6. D. Acharyya and P. Bhattacharyya, *Solid. State. Electron.*, 2015, **106**, 18-26.
7. L. Sui, X. Zhang, X. Cheng, P. Wang, Y. Xu, S. Gao, H. Zhao and L. Huo, *ACS Appl. Mater. Interfaces*, 2017, **9**, 1661-1670.
8. F. Qu, H. Jiang and M. Yang, *Nanoscale*, 2016, **8**, 16349-16356.
9. C. Sun, X. Su, F. Xiao, C. Niu and J. Wang, *Sens. Actuators, B*, 2011, **157**, 681-685.
10. J. Huang, X. Xu, C. Gu, W. Wang, B. Geng, Y. Sun and J. Liu, *Sens. Actuators, B*, 2012, **173**, 599-606.

11. Z. Lin, J. Gong, P. Fu, *J. Mater. Sci.: Mater. Electron.*, 2017, **28**, 4424-4430.
12. F. Li, Q. Qin, N. Zhang, C. Chen, L. Sun, X. Liu, Y. Chen, C. Li and S. Ruan, *Sens. Actuators, B*, 2017, **244**, 837-848.
13. F. Li, Y. Li, F. Jing, J. Zhou, Y. Chen, D. Sun and S. Ruan, *RSC Adv.*, 2015, **5**, 85598-85605.
14. F. Qu, B. Zhang, X. Zhou, H. Jiang, C. Wang, X. Feng, C. Jiang and M. Yang, *Sens. Actuators, B*, 2017, **252**, 649-656.
15. N. Zhang, Q. Qin, X. Ma, J. Zhou, L. Sun, C. Chen, S. Wen, Y. Chen and S. Ruan, *J. Alloys Compd.*, 2017,**723**, 779-786.
16. R. Xu, N. Zhang, L. Sun, C. Chen, Y. Chen, C. Li and Ruan S., *RSC Adv.*, 2016, **6**, 106364-106369.
17. K. Xu, J. Zou, S. Tian, Y. Yang, F. Zeng, T. Yu, Y. Zhang, X. Jie and C. Yuan, *Sens. Actuators, B*, 2017, **246**, 68-77.
18. Y. Li, F. Li, C. Li, W. Wei, D. Jiang, L. Zhu, D. Sun, X. Zhang and S. Ruan, *RSC Adv.*, 2015, **5**, 61528-61534.
19. L. Zhu, D. Zhang, Y. Wang, C. Feng, J. Zhou, C. Liu and S. Ruan, *RSC Adv.*, 2015, **5**, 28105-28110.